A Novel Geopolymer Foam Based On ZSM-5 Zeolite Fabricated Using Templating Emulsion/Chemical Foaming Method and Its Application in Batch and Continuous Dye Removal Systems

Mahboobeh Monjezi
ACECR Institute of Higher Education
Vahid Javanbakht (v.javanbakht@ce.iut.ac.ir)
ACECR Institute of Higher Education

Research Article

Keywords: Geopolymer foam, ZSM-5 zeolite, Dye removal, Adsorption

Posted Date: January 7th, 2022

DOI: https://doi.org/10.21203/rs.3.rs-1227901/v1

Abstract

Geopolymers as sustainable and environmentally friendly “green materials”, can be synthesized by utilizing waste material and by-products. A porous geopolymer foam adsorbent based on ZSM-5 zeolite was prepared using templating emulsion/chemical foaming method in different conditions and used for dye removal in batch and continuous systems. The parameters affecting the dye adsorption including temperature, concentration, and pH, kinetics, isotherm, and thermodynamics of the process were investigated. The results of the geopolymer foam synthesis showed that thermal pretreatment of the zeolite has a positive effect on the strength and adsorption capacity. Moreover, the increase in sodium silicate more than the stoichiometric reduces the strength and adsorption capacity. The findings obtained from the batch adsorption process showed that the adsorption kinetics of the pseudo-second-order model and the adsorption isotherm of the Temkin model is adjusted with the experimental data. Thermodynamic results indicated that the process of dye adsorption with geopolymer foam is exothermic. The results from continuous experiments indicated more compatibility of the adsorption process with the models of Thomas and Bohart-Adams. The maximum adsorption capacity of methylene blue in batch and continuous processes was 9.82 and 8.17 mg/g. The adsorbent reduction was performed successfully by chemical and thermal processes.

1. Introduction

With the growing population and industrialization, the release of effluents from different industries because of their adverse effects poses a serious threat to living organisms [1–10]. Dye effluents are among the most important environmental pollutants. Dyes have significantly different applications in industries like textiles, paper, plastics, rubber, concrete, and medicine. The textile industry is the main consumer of dyes completely harmful to the environment. Dispersion of dye molecules in the environment, block sunlight from reaching most of the damaged water system and thus reduce the level of dissolved oxygen (DO) in the water. Dyes may also increase the need for biochemical oxygen demand (BOD) in the contaminated water [11–16]. The level of toxicity of a particular dye is very important given its diverse effects on the environment and living organisms. Examining the harmful effects of dye compounds and their metabolites is very important to develop strategies to reduce their acute toxic effects. While some dyes do not have significant acute toxicity, several dyes, especially azo dyes, are carcinogenic. Most common carcinogens like benzidine are found in most dyes and must be purified before discharge. Commercially, azo dyes are of the most important classes of pigments that are used given their higher strength in production, easy preparation, availability of cheap raw materials, ability to cover the whole, and good strength properties. Besides dyes, there may be other contaminants like metals and auxiliaries used to produce dyes. Recently, a study has been reported on the estrogenic and anti-estrogenic activity of textile dyes, supporting the harmful effects of dyes on living organisms. Different approaches have been studied for removing dye from effluents, among which adsorption is considered as one of the most effective and simple methods [17–23]. Moreover, the vast majority of the studies focus on using powder adsorbents, which are not easily recoverable and therefore cannot be used in proper

applications or directly in packaging. Powder adsorbents may need the use of supporting materials (for instance porous ceramics, polymer foams) to allow industrial use or separation (for instance filtration) after the wastewater treatment process, both of which damage the sewage. Thus, using non-powder adsorbents with a porous substrate like geopolymers has been considered as an adsorbent. Geopolymers are produced by the reaction of aluminosilicate raw materials (metakaolin, fly ash, waste glass, and so on) with highly alkaline activators. Geopolymer foams have a wide range of properties like high mechanical strength, long durability, low thermal conductivity, good chemical, and thermal stability, and given their more environmentally friendly nature, they are a better choice than many materials proposed as synthetic chemicals adsorbents, filters, catalysts and environmentally friendly materials [24]. Zeolite is a mineral mainly composed of aluminosilicate whose main commercial application in industry is as a surface adsorbent. Their properties rely to some extent on the ratio of aluminum to silicon [25, 26]. ZSM-5 zeolite is a porous fine material widely used in chemicals applications like decomposition used as adsorbents. ZSM-5 is an alumina silicate zeolite that belongs to the pentazyl zeolite family. This material is the base of most industrial catalysts in the oil and petrochemical industries. It has been known that the efficiency and selection of a porous catalyst depend on their textural and structural properties and, more precisely, on the number of active sites on the external surface about the number of sites accessible through the porous system.

In this study, a novel geopolymer foam adsorbent based on pretreated ZSM-5 zeolite was prepared using templating emulsion/chemical foaming method, characterized, and then used to remove methylene blue dye from aqueous solutions. Experiments were done in batch and continuous systems. Kinetics, thermodynamics, and regeneration experiments, and the effect of different parameters on dye removal were investigated.

2. Materials And Methods

2.1 Materials

The chemicals used in the study were from analytical grade. Sodium silicate pentahydrate was obtained from Kimia Tejarat Fajr Company, potassium hydroxide and hydrogen peroxide were purchased from Mojallali Co., and ZSM-5 zeolite prepared from Petro Mehr Iran Co.

2.2 Synthesis of geopolymer foam based on ZSM-5 zeolite

The commonest synthesis method for producing geopolymer foams is by mixing a foaming agent (like hydrogen peroxide and metal powders) in the geopolymer slurry, which is usually called chemical foaming. This strategy utilizes the foaming agent reactions in the alkaline environment, as well as the alkaline activation of aluminosilicate precursors. This process produces gas bubbles trapped inside the slurry during adjustment, forming cavities in the hardened body. The emulsion templating method is another method examined for the synthesis of geopolymer foams where the geopolymer slurry is mixed with organic oil and results in the production of emulsion. The curing process creates a soap-making reaction to produce soap and water-soluble glycerol molecules. These products are then extracted (e.g.,

the water washing step) to produce porous geopolymers. Here, both methods were used in combination to prepare the adsorbents. First, the materials were calculated based on stoichiometric calculations. 13.9 g of sodium silicate with 7 ml of water at 50°C was placed on the stirrer for 30 minutes to get a gel-like mixture. Then 10 g of potassium hydroxide was mixed with 5 ml of distilled water and added to the sodium silicate mixture and stirred at room temperature for 15 minutes. Then 20 g of ZSM-5 was gradually added to the mixture and stirred with a mechanical stirrer at 1000 rpm until a uniform gel-like mixture was obtained. Then 2 mL of sunflower oil was added to the mixture gradually and stirred at 1000 rpm for 5 minutes. Finally, 5 mL of hydrogen peroxide, was added gradually and stirred at 1000 rpm for 5 minutes. The geopolymer foams were produced by casting the slurry into a sealed polystyrene mold and curing for 24 h at room temperature and another 24 h at 70°C in an oven. The preheat treatment can contribute to improving the physical strength and the rate of geo-polymerization. After completing the curing and polymerization reaction, the resulting foam dried at 70°C in the oven for 24 h and then placed in a furnace at 300°C for two hours. For the acid leaching process, the obtained foams were then placed in 3 M hydrochloric acid for one hour and finally washed with distilled water five times and dried at room temperature for 24 hours. Then 0.02 g of each sample was kept in 100 ml of distilled water for 4 days to examine the stability and durability in the water of the produced samples. Furthermore, 0.02 g of the foam in 20 ml of methylene blue dye solution was exposed for 2 hours in a continuous process at ambient temperature at 200 rpm for initial estimation of the ability of the adsorbent to adsorb the dye. The experiments were performed with different conditions from the initial compounds according to Table 1 with crude and pretreated zeolite which activated and calcined in an oven at 800°C for 2 hours.

Table 1
The geopolymer foams produced in different condition

Samples	Sodium silicate (g)	Potassium hydroxide (g)	Crude zeolite (g)	Pretreated zeolite (g)	Oil (mL)	Hydrogen peroxide (mL)
S1	13.9	10	0	20	0	5
S2	13.9	10	20	0	0	5
S3	13.9	10	0	20	2	5
S4	13.9	10	20	0	2	5
S5	16	10	20	0	2	5
S6	13.9	10	10	0	2	5

2.3 Characterization

Investigation of surface characteristics was performed by Field Scanning Electron Microscopy (FESEM-MIRA3). Fourier Transform Infrared Spectrometer (FTIR-AVATAR) was used to identify the functional groups. X-ray Diffraction (XRD-PW1730) was used to identify the structural properties of particles. Measurement of the specific surface area was performed by nitrogen adsorption-desorption analysis (BET-BELSORP MINI II). Thermogravimetric analysis (TGA) was performed by the TGA device (Q600

model, TA Company). UV-Spectrophotometer (RAYLEIGH UV-2601) was used to measure the concentration of dye solutions.

2.4 Zero-point charge determination

Zero-point charge (pHzpc) is an important property of the adsorbents, defined as the pH value where the net charge of the surface is zero showing the adsorbent surface at which pH is electrically neutral. To measure the pH_{ZPC}, 0.01 M NaCl solutions were prepared the pH of the solutions was adjusted in the range of 2 to 12 by 0.1 M hydrochloric acid and sodium hydroxide solutions, and then 0.05 g of the adsorbent added in 10 ml of the solution. The solutions were placed at room temperature for 48 hours and the pH of the solutions was measured again. The deviation in pH values was plotted in terms of initial pH.

2.5 Batch adsorption kinetic experiments

The batch adsorption kinetic experiments were performed to reach the equilibrium time. 0.05 g of the prepared adsorbent was placed in 50 mL of 10 mg/L methylene blue solution and placed in a shaker at 25°C and 200 rpm. At times 5, 10, 20, 30, 40, 60, 80, 120, 240, 1380, 1600, 1650, 2400 minutes, the solution was sampled at the specified time and analyzed with UV-spectrophotometer. The dye adsorbed on the adsorbent at time t (q_t in mg/g) and equilibrium (q_e in mg/g) were determined using the formula below:

$$q_t = \frac{\left(C_0 - C_t\right)V}{m}$$

1

$$q_e = \frac{\left(C_0 - C_e\right)V}{m}$$

2

where, C_0 is the initial concentration of the solution (mg/L), C_t is the concentration at time t (mg/L), V is the volume of solution (L), and m is the adsorbent mass (g).

2.7 Adsorption isotherm experiments

Isotherm tests were performed to determine the effect of temperature and concentration on adsorption and to examine thermodynamic studies at 25 and 40°C. In this test, 20 mL of dye solutions with concentrations of 2, 4, 6, 8, 10 mg/L of methylene blue were prepared and 0.02 g of absorbent was placed in each of the solutions in a shaker for 25 hours at 25 and 40°C. Then the samples were taken out of the shaker and after sampling them, analyzed with UV-spectrophotometer.

2.8 Adsorbent regeneration and reuse experiments

The adsorbent reduction was performed by two methods to reuse it: acidic and heating reduction. In the acidic method, the reduction was done using 0.2 M hydrochloric acid solution and in the other method by heating in a furnace, both of which were repeated in four steps. In both methods, 0.05 g of the adsorbent was placed in 50 mL of 10 mg/L methylene blue solution and a shaker for 2 hours. After the adsorption process, the adsorption capacity was measured by UV-spectrophotometer. The adsorbent was separated from the solution and then placed in the hydrochloric acid solution for 30 minutes to regenerate and remove the adsorbed dyes. Then it was rinsed five times with distilled water and the previous process was continued again and each time it was done with a new methylene blue solution. In the heating reduction by furnace done on another adsorbent, the used adsorbent was placed in a furnace at 800°C for two hours after each adsorption process and the previous processes were repeated.

3. Results And Discussion

3.1 The results of synthesis of the geopolymer foams

The whole preparation was simple, and the overall cost was lower than that of traditional commercial inorganic adsorbents. The geo-polymerization mechanism for the zeolite-based geopolymer is that a polycondensation of [AlO_4] and [SiO_4] groups occurred to form polymer gels with three basic structural units in the hydration layer of the hydrated sodium ions during the condensation polymerization process; this layer was located at the interface between the solid and the liquid in the initial gel [27]. The geopolymer foams were prepared and evaluated using various initial conditions. Given the results in Table 2, examining the effect of raw material composition on the fabricated geopolymer foams showed that increasing sodium silicate more than the calculated stoichiometric value reduces the strength and the dye adsorption. On the other hand, thermal processing (activation) of the zeolite has a positive effect on the strength and adsorption capacity of the adsorbent foam. The results showed that the chemical foaming method resulted in greater strength of the final structure compared to the emulsion templating method with a positive effect on the dye adsorption capacity. By comparing the values related to strength and the ability of the adsorbent foam to absorb the dye, finally, sample 3 was selected as the optimal sample for further adsorption investigations.

Table 2
Examining the effect of raw material composition on geopolymer structure

Samples	Synthesis method	Sample density (g/mL)	Durability in water (day)	Dye adsorption (mg/g)
S1	Chemical foaming	0.0087	4	1.95
S2	Chemical foaming	0.0020	3	1.72
S3	Templating Emulsion/Chemical foaming	0.0126	4	2.69
S4	Templating Emulsion/Chemical foaming	0.0075	3	2.62
S5	Templating Emulsion/Chemical foaming	0.0080	2	2.04
S6	Templating Emulsion/Chemical foaming	Not produced	-	-

3.2 Analysis of the prepared geopolymer adsorbent

3.2.1 FESEM analysis results

The photograph and FESEM results of the surface structure and cross-sectional view of the prepared geopolymer adsorbent foam are shown in Fig. 2 for morphologic investigation. As shown in Fig. 2, the geo-polymerization reaction causes the formation of a series of macropore structures due to the bursting of bubbles formed by the hydrogen peroxide reaction in the geopolymer substrate:

$$2H_2O_2(l) \rightarrow 2H_2O(l) + O_2(g) \uparrow$$

4

Figures illustrate that geopolymer foam has high porosity and many pores with relatively uniform size distribution.

3.2.2 XRD analysis results

Figure 3 represented the XRD results and phase structure of the ZSM-5 zeolite and prepared geopolymer foam. By comparing the X-ray diffraction pattern of the foam created concerning the raw zeolite, it is found that the primary zeolite has a crystalline structure with sharp peaks, whereas the foam produced has an amorphous polymeric structure without the initial sharp peaks which is a representation of the geo-polymerization process to form the desired foam. The main feature was obtained by XRD measurements from the very broad reflection between 2θ = 15 and 35° assigned to an amorphous phase with the presence of a small number of trace minerals. The differences in the 2θ position of the broad reflection in the XRD patterns for zeolite and geopolymer foam provided evidence for the dissolution of SiO4 and AlO4− species from zeolite in the alkaline environment during the geo-polymerization reaction

[28]. The sharp reflections due to the residual crystalline phases such as quartz were also observed alongside the broad reflection.

3.2.3 XRF analysis results

The chemical composition of the samples was determined by XRF and is shown in Table 1. Given the results, the presence of sodium and potassium components participating in the geo-polymerization reaction in the resulting foam can be confirmed.

Table 3
Chemical composition of ZSM-5 and zeolite-based geopolymer

Sample	Chemical composition				
	SiO_2	Na_2O	K_2O	Cl	Al_2O_3
ZSM-5 zeolite	97.03	-	-	-	1.72
Geopolymer foam	60.87	11.77	10.52	2.45	0.88

3.2.4 TGA analysis results

TGA analysis was done to evaluate the thermal stability of the foam. Fig. 4 shows that there are three distinct steps in weight loss. Firstly, about 6 to 8% weight loss at 100°C took place because of water evaporation. As the processes of adsorption of most aqueous pollutants are done at temperatures below 100°C and ambient temperature, this weight loss shows the appropriate thermal stability of the adsorbent for these applications. Then the significant weight loss of 15% occurs between 100 to 400°C that may be because of the decomposition of the geopolymer adsorbent. Stabilization in the temperature range of 400 to 800°C occurred that showed an overall weight reduction of about 20% from 30°C to 800°C, showing geopolymer foam is stable at high temperatures.

3.2.5 BET analysis results

Figure 5 shows the BET analysis diagrams for the geopolymer foam. Based on the diagrams, the isotherm is an IV-type isotherm. This type of isotherm is used for porous materials. If the P/P_0 ratio is low, it is similar to the type II isotherm, but when this ratio is very large, the material has very narrow, capillary pores, where the adsorption rate increases significantly and the adsorbent material condenses on the surface. This type of isotherm is usually seen for industrial catalysts and the corresponding curve is used to determine the pore size distribution. Furthermore, hysteria is seen in this type of isotherm. Hysteresis shows the presence of meso cavities in the material and can be used to obtain information about the geometry of the cavities.

BET analysis was used to investigate the behavior of nitrogen molecules in the adsorption phenomenon on the adsorbent surface and calculate the specific surface area, total pore volume, and average pore diameter of the adsorbent. According to the BET results, the specific surface area, total pore volume, and

average pore diameter of the prepared adsorbent foam were 4.41 $m^2.g^{-1}$, 0.01 $cm^3.g^{-1}$, and 9.62 nm, respectively.

3.2.6 Determination of zero-point charge results

For the Determination of zero-point charge, the graph of (pHf-pHi) vs pHi was plotted as shown in Fig. 6. The intersection of the curve with the horizontal line is known as the endpoints of the pH_{ZPC} and this value is about pH =10 for the adsorbent. At high pH values (pH> pH_{ZPC}), the adsorbent surface is negatively charged, and the adsorption of dye molecules increases because of the electrostatic adsorption between the surface and the cationic dye molecules. At low pH values (pH <pH_{ZPC}), as the adsorbent surface, is positively charged, the expected tendency is to reduce the dye adsorption because of the electrostatic repulsion between the cationic dye molecules and the adsorbent surface [29].

3.3 The results of the methylene blue adsorption by the geopolymer adsorbent

3.3.1 Batch adsorption kinetics

Batch adsorption tests were performed to examine the adsorption kinetics and reach equilibrium time. Fig. 7 indicates the concentration decay of methylene blue over time. The concentration of methylene blue decreases over time, and the adsorption rate decreases as the curve slope. Over time, the value of adsorbed dye increases, and the active sites on the adsorbent surface occupy with dye molecules until approaching the adsorption equilibrium. Adsorption capacity in the equilibrium state was calculated to equal 9.82 mg/g for 10 mg/L initial concentration. The results of the study of kinetic models of pseudo-first-order, pseudo-second-order, Elovich, and intraparticle diffusion are given in Table 4. The proximity of the correlation coefficient (R^2) to 1 shows less deviation and more accuracy of the model. According to R^2 values, the models were well-fitting to the experimental data but, the pseudo-second-order model has the best adjustment. Given the obtained R^2 and the proximity of the obtained adsorption capacity with its experimental value as shown in the figure, one can state that the adsorption process was consistent with the pseudo-second-order kinetic model. In the intraparticle diffusion model $K_{i,1} > K_{i,2} > K_{i,3}$ examines the adsorption steps on the outer surface, inner section, and equilibrium. In the first stage, the molecules of the adsorptive must be transferred from the solution bulk to the adsorbent surface. The adsorbed molecules must pass through the solution boundary layer that surrounds the adsorbent particle, called film diffusion. In the second stage, the adsorbed molecules must penetrate the adsorbent pores. In the last stage, the particle must be attached to the adsorbent surface, which eventually reaches equilibrium.

Table 4. The Linear form of different kinetics models, and the parameters related to different kinetics models for methylene blue adsorption

Batch kinetic models	Equation
Pseudo-first-order	$Ln\ (q_e - q_t) = Ln\ q_e - k_1 t$
Pseudo-second-order	$\frac{t}{qt} = \frac{1}{k2qe2} + \frac{t}{qe}$
Elovich	$q_t = \frac{1}{\beta} Ln\ (\alpha\beta) + \frac{1}{\beta} Lnt$
Intraparticle diffusion	$q_t = k_i t^{0.5} + C$

Pseudo-first-order			Pseudo-second-order		
K_1(1/min)	q_e (mg/g)	R^2	K_2(g/mg.min)	q_e (mg/g)	R^2
0.0016	5.29	0.9141	0.0025	9.74	0.9985

Elovich			Intra-particle diffusion		
α(mg/g.min^{-1})	β(g/mg)	R^2	K_1 (mg/(g.min$^{0.5}$))	K_2 (mg/(g.min$^{0.5}$))	K_3 (mg/(g.min$^{0.5}$))
0.898	0.774	0.9415	1.297	0.1403	0.036

Continuous kinetic models	Equation
Bohart-Adams	$Ln\left(\frac{C_t}{C_0}\right) = K_{AB}C_0 t\ - K_{AB}N_0\frac{Z}{F}$
Thomas	$\frac{C_t}{C_0} = \frac{1}{1 + \exp\left(\frac{k_{TH}q_m M}{Q} - k_{TH}C_0 t\right)}$
Yoon-Nelson	$Ln(\frac{Ct}{C_0 - Ct}) = K_{YN}t - \tau K_{YN}$

C_0 (mg/l)	Bohart-Adams			Thomas			Yoon-Nelson		
	K_{AB} (L/mg.min)	N_0 (mg/L)	R^2	K_{TH} (mL/min.g)	q_m (mg/g)	R^2	K_{YN} (L/min)	τ (min)	R^2
5	0.0062	1.574	0.9412	0.0109	4.396	0.9551	0.058	4.32	0.9551
10	0.0021	5.338	0.7542	0.004	17.325	0.9459	0.0408	3.686	0.9458

3.3.2 Continuous adsorption kinetics

The results of the investigation of the effluent solution from the continuous adsorption column (Fig. 8) indicated that over time the dye concentration inside the column increased, which shows that dye adsorption decreased because the adsorbent active sites were saturated by the dye molecules over time. Adsorption capacity in equilibrium state and column saturation was calculated using equation 3 equal to 5.38 and 8.17 mg/g for 5 and 10 mg/L initial concentration, respectively. The adsorption process of

methylene blue was investigated using the Thomas, Bohart-Adams, and Yoon-Nelson models, and the adsorption conformity to each model is represented in Table 4. Investigation of the correlation coefficients led to the conclusion that the Thomas and Yoon-Nelson models have the best fitting which states that adsorption of the adsorbate on the adsorbent occurs directly, meaning that the adsorption rate is controlled by the surface reaction between the adsorbate and the unoccupied capacity of the adsorbent.

3.3.3 Investigation of methylene blue adsorption isotherm by geopolymer adsorbent

Adsorption isotherm is one of the most important factors in designing adsorption systems. Indeed, the adsorption isotherm explains how the adsorbent and the adsorbate interact. Thus, it is always considered as a basic factor in determining the adsorption capacity and optimize the adsorbent consumption. The equilibrium of the adsorption process is usually shown by matching experimental data with different isotherm models such as Langmuir, Freundlich, and Temkin models. The models were plotted (Fig. 9) and the results were represented in Table 5. Investigation of the R^2 led to the conclusion that the adjusted models were consistent with the experimental data and the Temkin model has the best fitting.

Table 5. Different isotherm models and their parameters

Model	Equation	Linear form	Model parameters
Freundlich	$q_e = K_F C_e^{\frac{1}{n}}$	$\log(q_e) = n\log(C_e) + \log(K_F)$	q_e (mg/g) C_e (mg/L) K_F ((mg/g) (L/mg)$^{1/n}$)
Langmuir	$q_e = \frac{q_m K_a C_e}{1 + K_a C_e}$	$\frac{C_e}{q_e} = \frac{1}{q_m} C_e + \frac{1}{q_m K_a}$	q_e (mg/g) C_e (mg/L) q_m (mg/g) K_a (L/mg)
Temkin	$q_e = \frac{RT}{b_T} \ln(A_T C_e)$	$q_e = \frac{RT}{b_T} \ln(C_e) + \frac{RT}{b_T} \ln(A_T)$	q_e (mg/g) C_e (mg/L) b_T (J/mol) A_T (L/g) R (8.314 J/mol K)

Freundlich

T (°C)	K_f	1/n	R^2
25	1.583	0.585	0.9522
40	0.819	0.206	0.8337

Langmuir

T (°C)	K_a	q_m	R^2
25	0.339	0.373	0.9895
40	0.077	9.825	0.7686

Temkin

T (°C)	A_T (L/g)	b_T (J/mol)	R^2
25	3.014	1637	0.9948
40	3.942	6347	0.9351

3.3.4 Examining of thermodynamics of methylene blue adsorption by geopolymer adsorbent

Thermodynamics is carried out to see if the process is endothermic and exothermic as well as spontaneous. In this study, Gibbs free energy (ΔG), enthalpy (ΔH), entropy (ΔS), and energy activation (E_a) were examined at temperatures of 298.15 and 313.15 K. The parameters intended were calculated by the Van't Hoff equation and plot (Fig. 10).

$$\log\left(\frac{q_e}{C_e}\right) = -\frac{\Delta H}{2.303R}\frac{1}{T} + \frac{\Delta S}{2.303R}$$

4

$\Delta G = \Delta H - T\Delta S$ (5)

$E_a = \Delta H + RT$ (6)

The results of the calculations of the desired parameters are shown in Table 6. Negative values of enthalpy, entropy and Gibbs free energy show the exothermicity, a reduction in irregularity, and spontaneity of the process, respectively.

Table 6
Thermodynamic parameters for methylene blue adsorption process

C_0 (mg/L)	T (K)	E_a (kJ/mol)	ΔG (kJ/mol)	ΔH (kJ/mol)	ΔS (J/mol.K)
2	298.15	45.622	-1.103	-48.121	-157.2
	313.15	45.51	1.262		
4	298.15	29.713	0.781	-32.192	-104.3
	313.15	29.589	-0.799		
6	298.15	27.445	0.025 -	29.924 -	-100.3
	313.15	27.321	1.479		
8	298.15	21.319	0.291	23.798-	-80.8
	313.15	21.194	1.503		
10	298.15	15.254	1.212	17.733-	-63.5
	313.15	15.130	2.165		

3.3.5 Examining the effect of various parameters on the adsorption of methylene blue dye

The effect of temperature

Given the adsorption data at various temperatures in Fig. 11a, the adsorption capacity has decreased with an increase in temperature. With the increase in temperature, the adsorption interaction between methylene blue molecules and active sites of the adsorbent decreases, which reduces the dye adsorption.

The effect of initial concentration

The initial concentration of the solution affects the adsorption. According to the results in Fig. 11a, the adsorption increases with an increase in concentration. This process can be explained by the improvement of the driving force that reduces the mass transfer resistance between the adsorptive and adsorbent. At higher concentrations, it provides a fundamental driving force to reduce the mass transfer resistance between the liquid and the solid phases.

The effect of pH

As a key element in adsorption, pH affects the chemical properties of the adsorbent and solution. Methylene blue is a cationic dye with a positive charge in the solution phase. Hence, methylene blue is an ionic species and its adsorption on the adsorbent surface is primarily affected by the adsorbent surface charge, affected by the pH of the solution. The effect of pH was examined in the range of 5 to 9 (Fig. 11b). As can be seen in the Figure, an increase in the percentage of removal dye was observed by both increasing and decreasing pH. At high pH values, the increase of the dye adsorption can be explained as the negative charging of the surface depending on the pHzpc value of the adsorbent. However, at low pH values, the reason for the dye adsorption value not decreasing can be explained as the replacement of the hydrogen ions on the adsorbent surface with the cationic methylene blue dye molecules in the solution. In an acidic medium, the initial pH value of adsorption firstly increases and then reaches an initial value by decreasing can be accepted as an indication of the previous situation.

3.3.6 Regeneration and reusing the adsorbent

Regeneration and reusing are very important in the adsorbent application. Two methods were used to reduce the adsorbent dye. As Fig. 11c shows, the adsorbents are still capable of adsorbing the dye after four cycles of regeneration and reusing, and in the acidic method, the adsorbent has shown better efficiency than the thermal method, which can be because of the adsorbent degradation in the furnace and thus decreasing its weight and as well as decreasing adsorption level.

3.4 Comparison of methylene blue adsorption capacity by the adsorbent and some similar adsorbents

Table 7 shows a comparison of the results of the maximum adsorption capacity of methylene blue from aqueous solutions compared to some similar adsorbents used. According to these data, the prepared adsorbent has a good adsorption capacity for methylene blue adsorption compared to the used adsorbents.

Table 7
Comparison of maximum methylene blue dye adsorption by different adsorbents

Adsorbent	Adsorption capacity (mg/g)	Ref.
Carbon/calcium/alginate	1.50	57
Magnetic cellulose	1.80	58
PAN-g-alginate	3.51	59
Polyurethane foam membranes	4.27	60
PMMA-g-alginate	5.25	61
H. cannabinus-g-PAA	7.11	62
Carboxymethyl sago pulp hydrogel	7.90	63
Activated CMC/potassium-carrageenan/montmorillonite	12.50	64
ZSM-5 zeolite based geopolymer foam	9.74	This study

4. Conclusion

In this research, a novel geopolymer foam adsorbent based on ZSM-5 zeolite was prepared using templating emulsion/chemical foaming method and characterized and then used to remove methylene blue dye from aqueous solutions. Experiments were done in batch and continuous systems. The parameters affecting the dye adsorption process including temperature, initial concentration, and pH of the solution were examined. Kinetics, isotherm, and thermodynamics of the adsorption process were studied. The results of the geopolymer foam synthesis showed that thermal pretreatment of the zeolite has a positive effect on the strength and adsorption capacity. Moreover, the increase in sodium silicate more than the stoichiometric reduces the strength and adsorption capacity. The findings obtained from the batch adsorption process showed that the adsorption kinetics of the pseudo-second-order model and the adsorption isotherm of the Temkin model is adjusted with the experimental data. Thermodynamic results indicated that the process of dye adsorption with geopolymer foam is exothermic. The results from continuous experiments indicated more compatibility of the adsorption process with the models of Thomas and Bohart-Adams. The maximum adsorption capacity of methylene blue in the batch and the continuous process was 9.82 and 8.17 mg/g. Therefore, the removal of dyes by the geopolymer foam adsorbent is an alternative to better use of wastewater treatment, being economically beneficial, and collaborating with the environment.

Declarations

Acknowledgment

Financial support of this work by the ACECR Institute of Higher Education (Isfahan Branch) is gratefully appreciated.

Conflict of interest

We have no conflict of interest to declare.

References

1. M.R. Sabouri, V. Javanbakht, D.J. Ghotbabadi, M. Mehravar, Process Safety and Environmental Protection (2019)
2. A. Banihashemi, V. Javanbakht, H. Mohammadifard, Mater. Chem. Phys. **258**, 123934 (2021)
3. M. Irandoost, M. Pezeshki-Modaress, V. Javanbakht, Journal of Water Process Engineering **32**, 100981 (2019)
4. F. Keyvani, S. Rahpeima, V. Javanbakht, Solid State Sci. **83**, 31–42 (2018)
5. M. Khadivi, V. Javanbakht, J. Mol. Liq. **319**, 114137 (2020)
6. S.I. Mohammadabadi, V. Javanbakht, Int. J. Biol. Macromol. **164**, 1133–1148 (2020)
7. S.I. Mohammadabadi, V. Javanbakht, Renewable Energy **161**, 893–906 (2020)
8. S.I. Mohammadabadi, V. Javanbakht, J. Mol. Liq. **315**, 113715 (2020)
9. R. Nowruzi, M. Heydari, V. Javanbakht, Int. J. Biol. Macromol. **147**, 209–216 (2020)
10. S. Rahpeima, V. Javanbakht, J. Esmaili, J. Inorg. Organomet. Polym Mater. **28**, 195–211 (2018)
11. V. Javanbakht, R. Shafiei, Int. J. Biol. Macromol. **152**, 990–1001 (2020)
12. F. Aeenjan, V. Javanbakht, Res. Chem. Intermed. **44**, 1459–1483 (2018)
13. K. Badvi, V. Javanbakht, Journal of Cleaner Production 280 124518
14. M. Bayat, V. Javanbakht, J. Esmaili, Int. J. Biol. Macromol. **116**, 607–619 (2018)
15. M. Erfani, V. Javanbakht, Int. J. Biol. Macromol. **114**, 244–255 (2018)
16. V. Javanbakht, M. Mohammadian, Journal of Molecular Structure (2021) 130496
17. M. Mehrabi, V. Javanbakht, J. Mater. Sci.: Mater. Electron. **29**, 9908–9919 (2018)
18. S. Mirzaei, V. Javanbakht, Int. J. Biol. Macromol. **134**, 1187–1204 (2019)
19. S.M.T.H. Moghaddas, B. Elahi, M. Darroudi, V. Javanbakht, J. Mol. Liq. **296**, 111834 (2019)
20. S.M.T.H. Moghaddas, B. Elahi, V. Javanbakht, J. Alloy. Compd. **821**, 153519 (2020)
21. Z. Vaez, V. Javanbakht, Journal of Photochemistry and Photobiology A: Chemistry (2019) 112064
22. N. Marsiezade, V. Javanbakht, Int. J. Biol. Macromol. **162**, 1140–1152 (2020)
23. M. Mahmoodi, V. Javanbakht, International Journal of Biological Macromolecules (2020)
24. C. Bai, T. Ni, Q. Wang, H. Li, P. Colombo, J. Eur. Ceram. Soc. **38**, 799–805 (2018)
25. V. Javanbakht, S.M. Ghoreishi, Adsorpt. Sci. Technol. **35**, 241–260 (2017)

26. V. Javanbakht, S.M. Ghoreishi, N. Habibi, M. Javanbakht, Protection of Metals and Physical Chemistry of Surfaces **53**, 693–702 (2017)
27. Y. Ge, Y. Yuan, K. Wang, Y. He, X. Cui, J. Hazard. Mater. **299**, 711–718 (2015)
28. E. Prud'Homme, P. Michaud, E. Joussein, C. Peyratout, A. Smith, S. Rossignol, Appl. Clay Sci. **51**, 15–22 (2011)
29. S.I. Mohammadabadi, V. Javanbakht, Ind. Crops Prod. **168**, 113575 (2021)

Figures

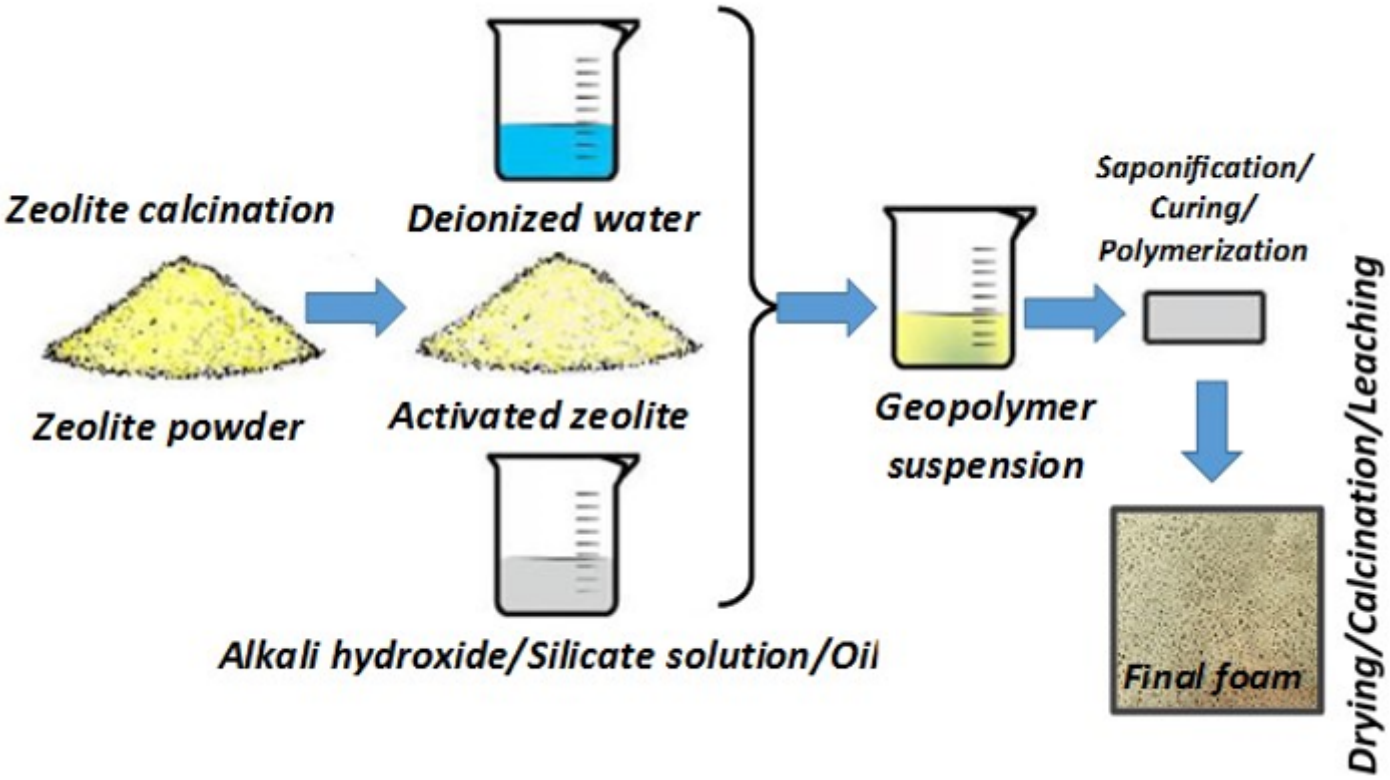

Figure 1

A schematic fabrication process of zeolite-based geopolymer foam

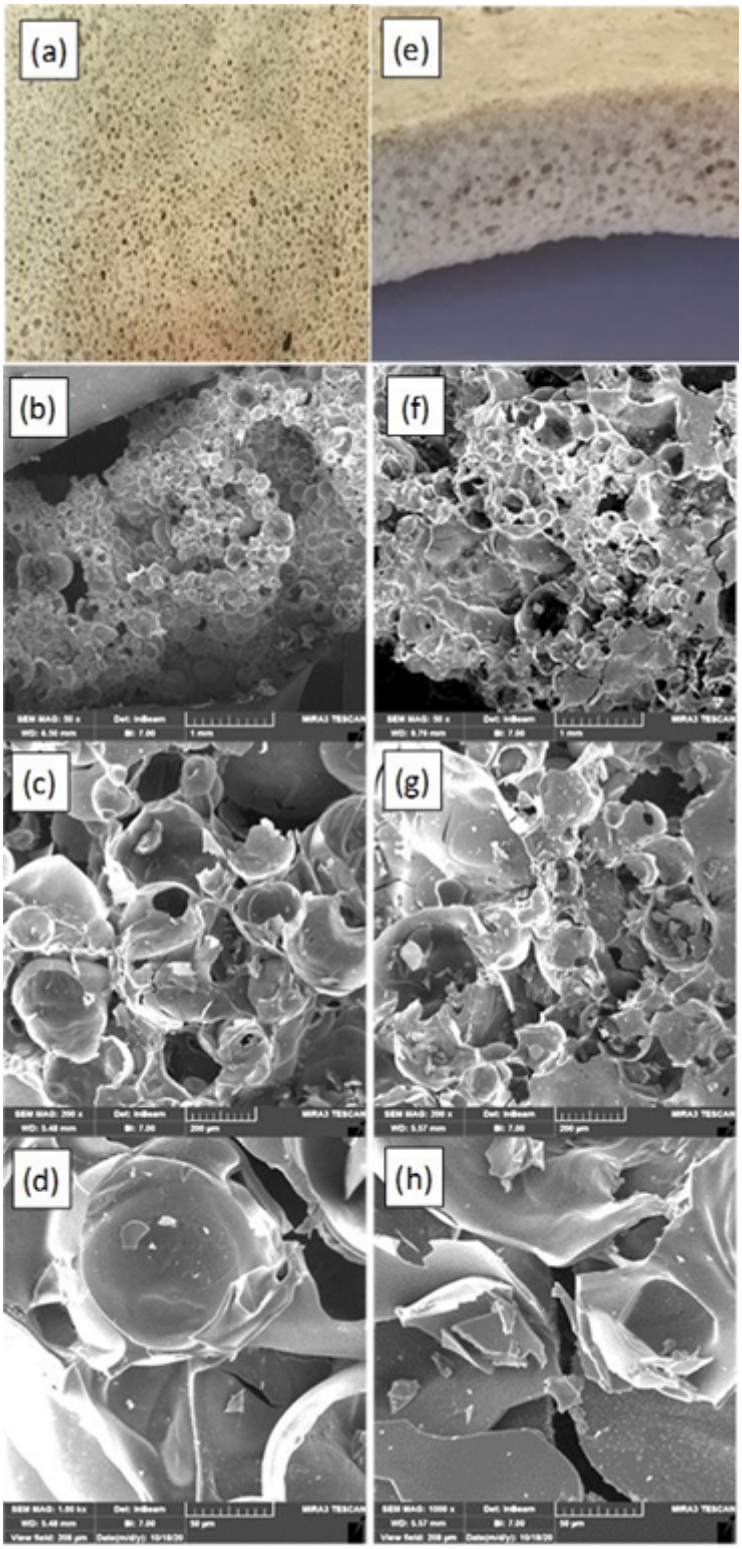

Figure 2

The photograph and FESEM results of (a-d) surface, and (e-h) cross-sectional view of the prepared geopolymer adsorbent foam, respectively

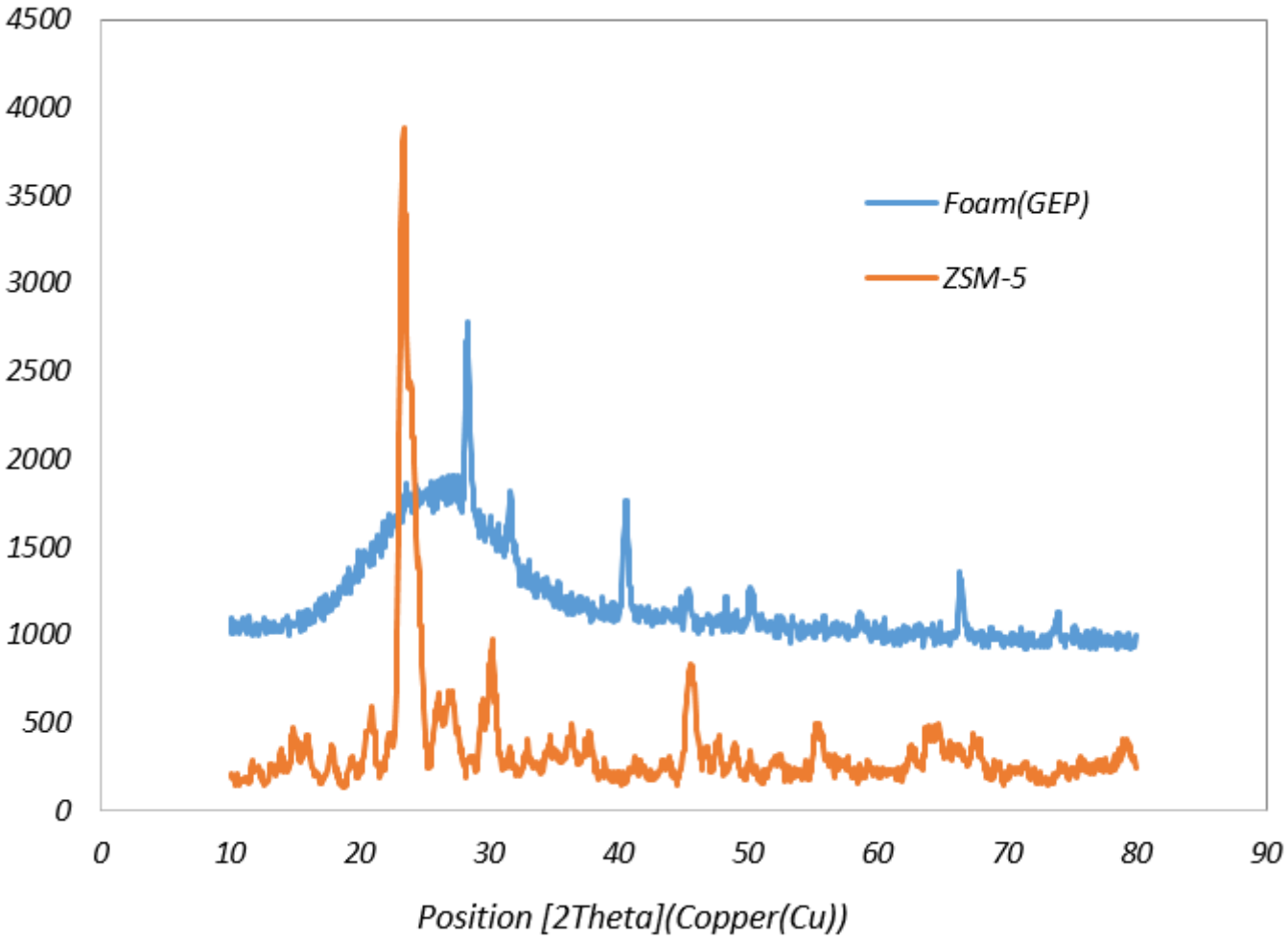

Figure 3

Comparison of XRD analysis results related to zeolite-based geopolymer and ZSM-5 zeolite

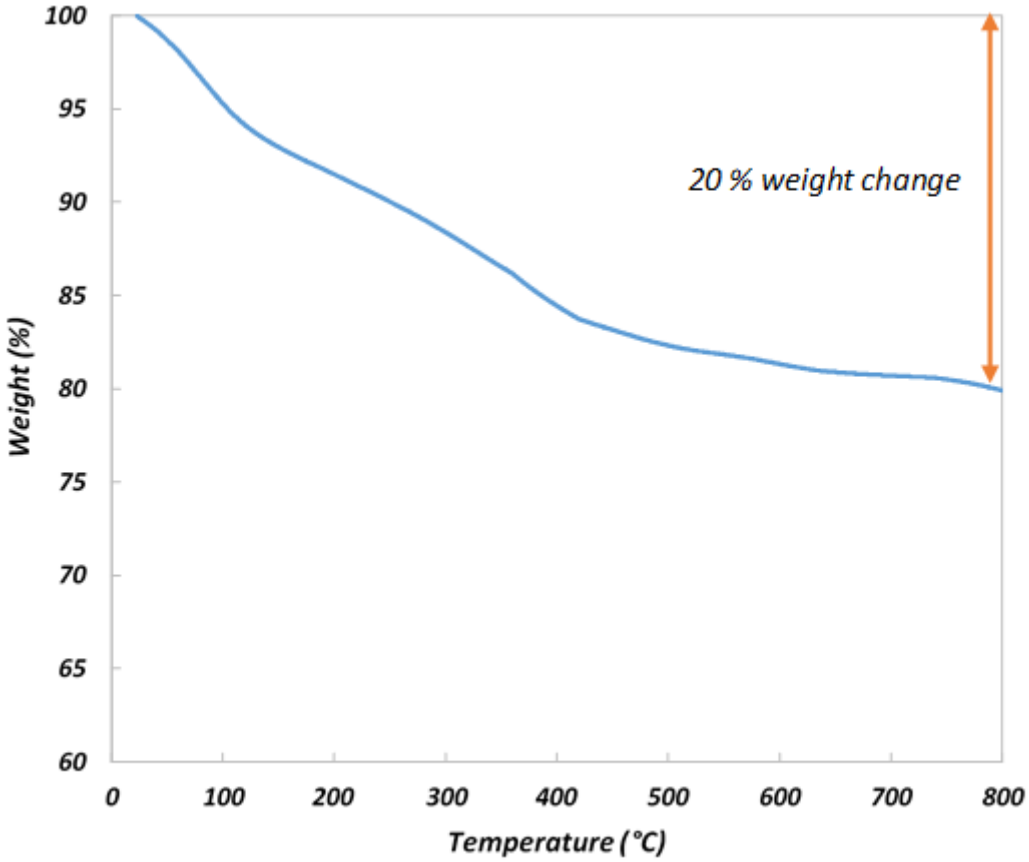

Figure 4

The results of TGA analysis related to the geopolymer foam

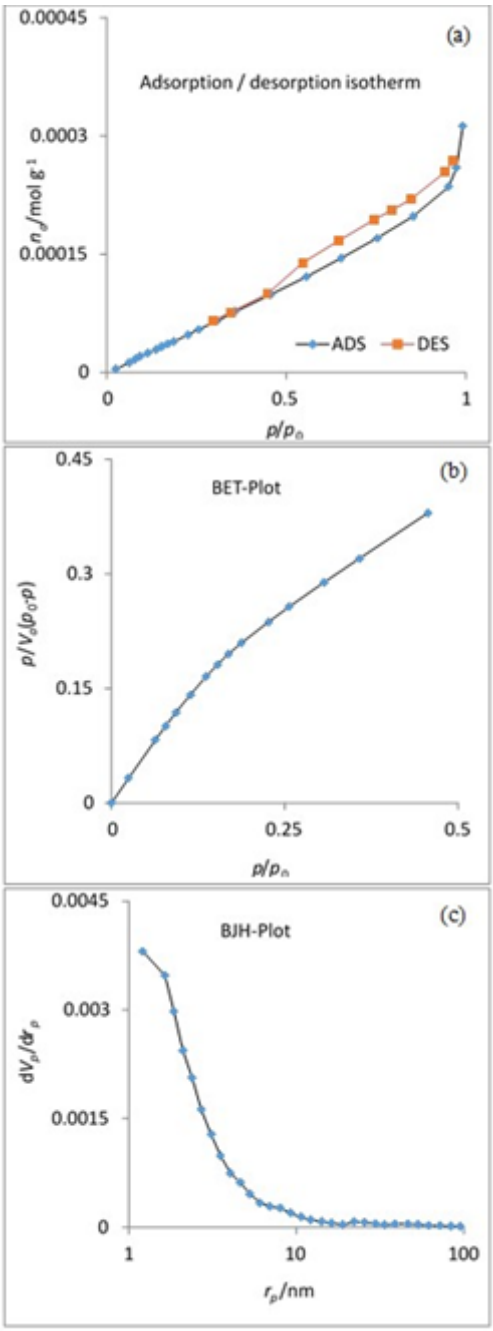

Figure 5

Adsorption/desorption isotherm diagrams of the geopolymer foam

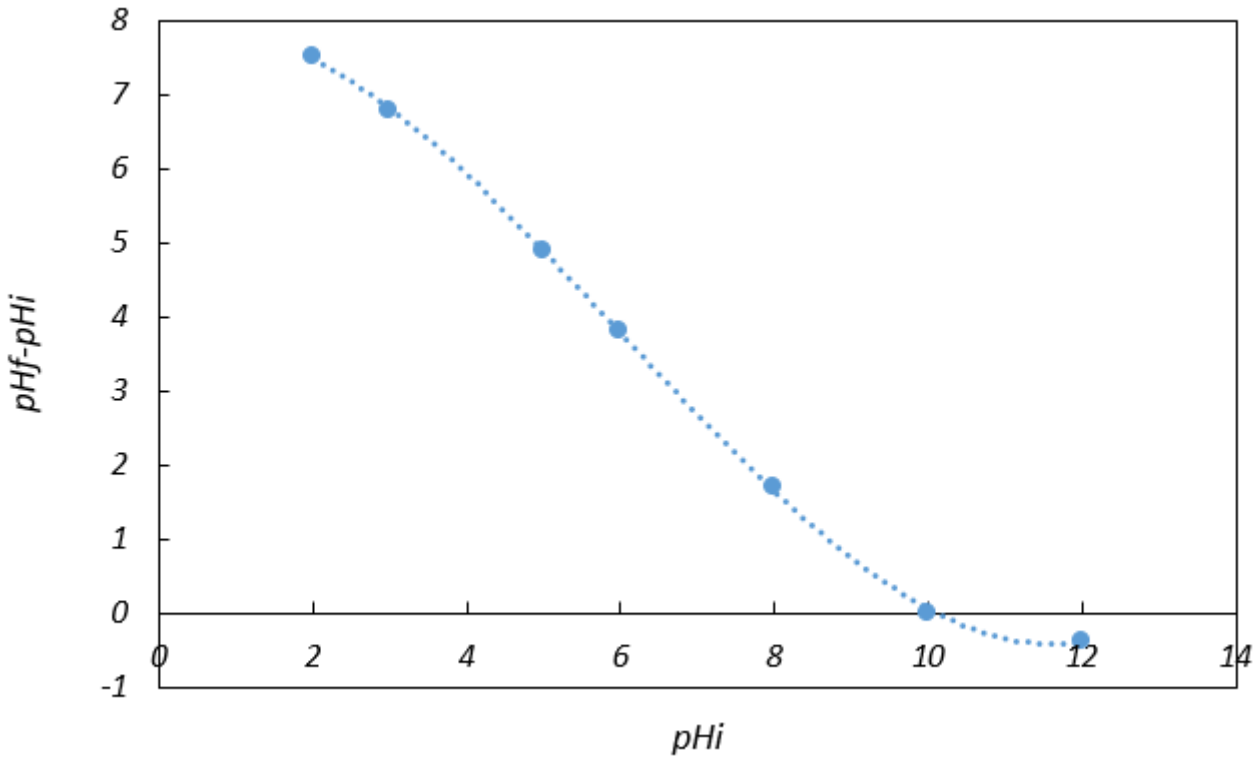

Figure 6

Plot for determination of point zero charge of the geopolymer foam

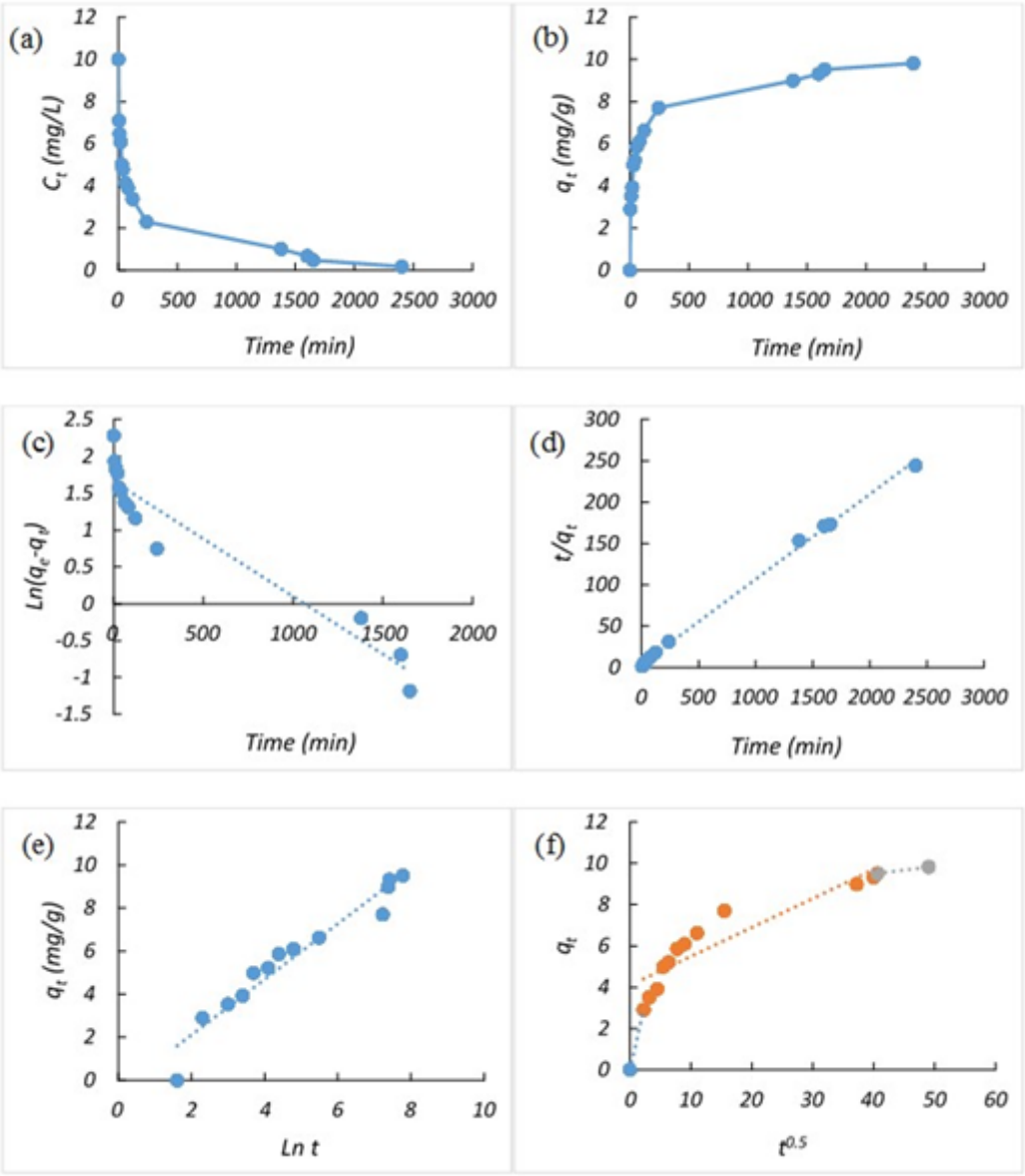

Figure 7

Changes in (a) methylene blue concentration and (b) adsorption over time, and adaptation of experimental data with (c) pseudo-first-order, (d) pseudo-second-order, (e) Elovich, and (f) intraparticle diffusion model for 0.05 g of the adsorbent in 50 mL of 10 mg/L methylene blue solution at different times in batch adsorption process

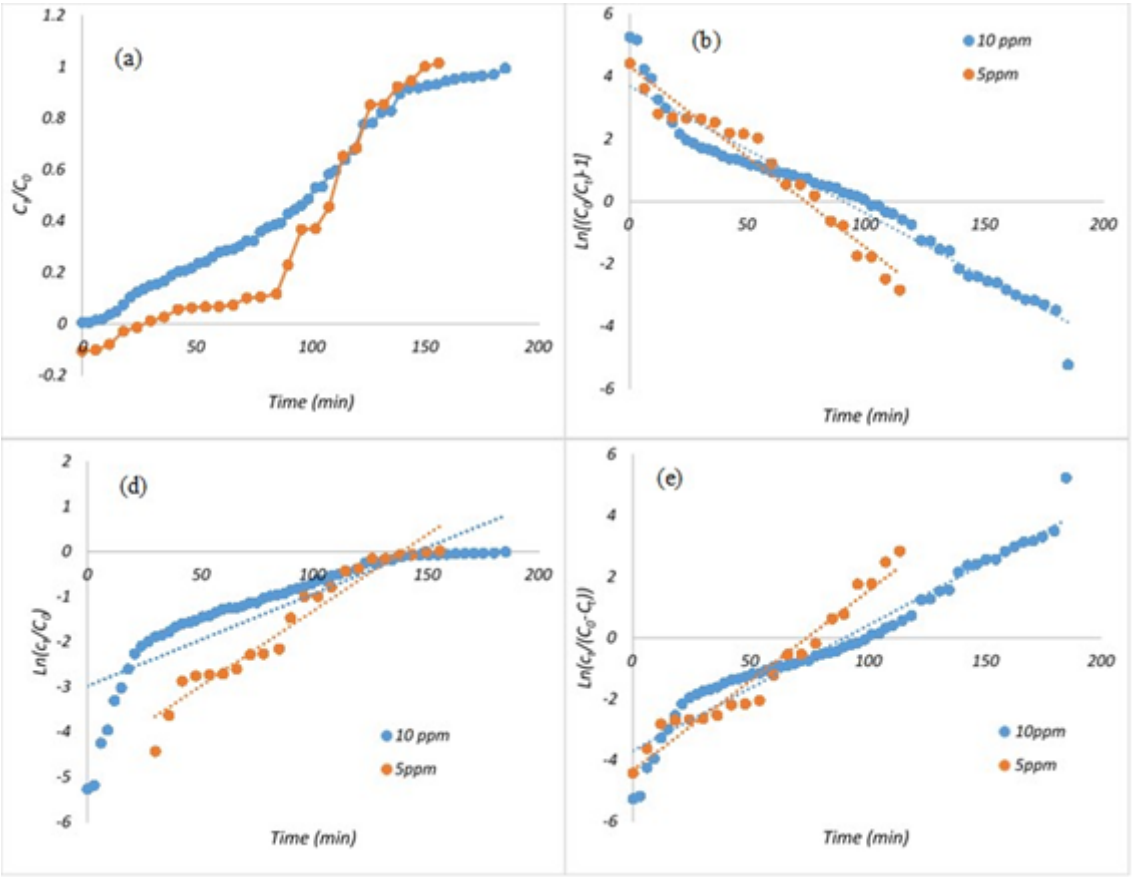

Figure 8

(a) Changes in methylene blue concentration over time, and adaptation of experimental data with (b) Thomas, (c) Bohart-Adams, and (d) and Yoon-Nelson models for 10 mg/L methylene blue solution at different times in continuous adsorption process

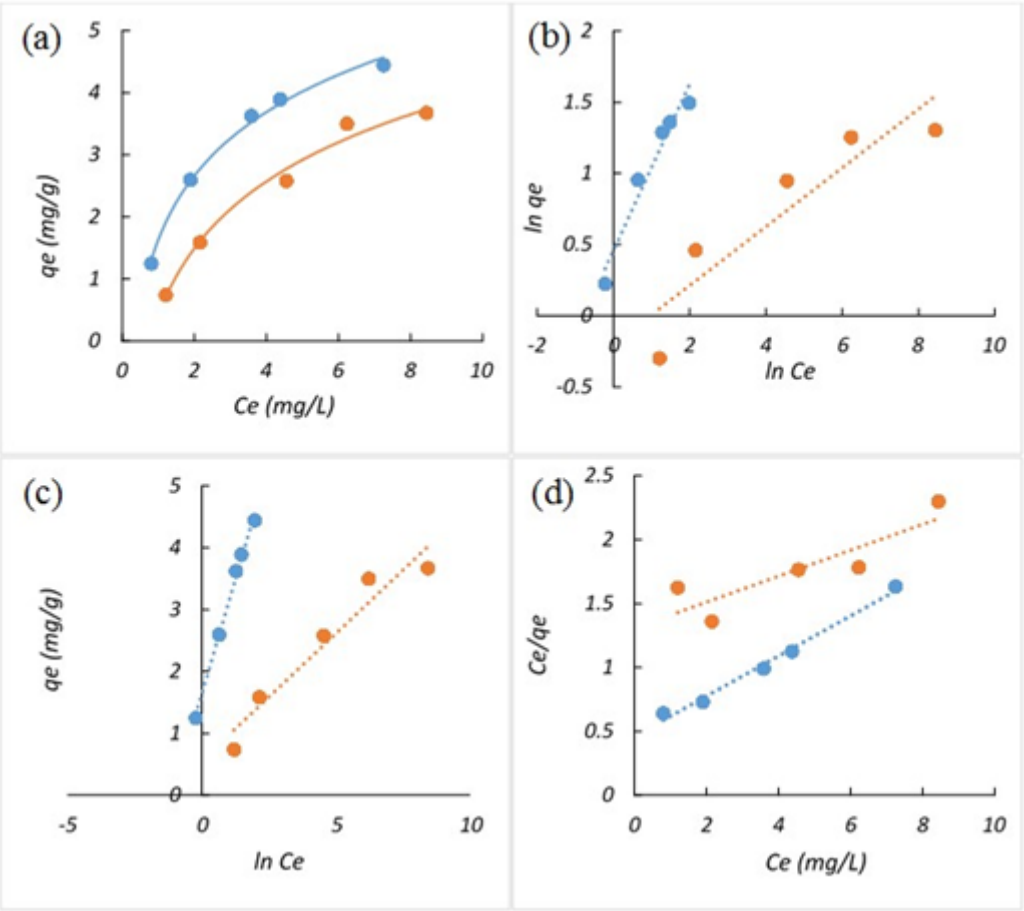

Figure 9

Methylene blue equilibrium adsorption isotherm at different temperatures for 0.02 of adsorbent in 20 mL of solution at various concentrations (a) and adaptation of isotherm data with Freundlich, Langmuir, and Temkin isotherm models

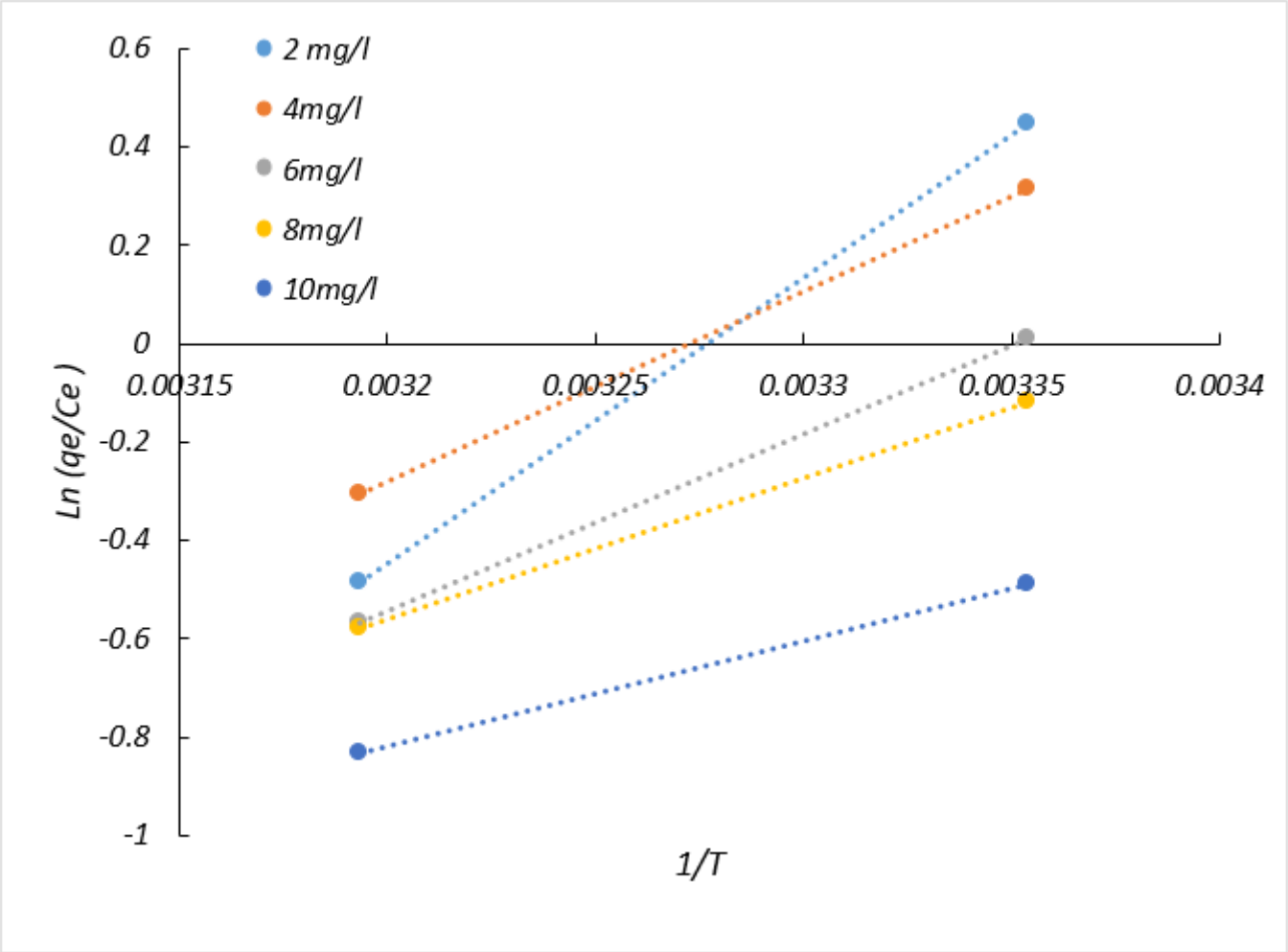

Figure 10

Van't Hoff equation plot for methylene blue adsorption for 0.02 of adsorbent in 20 mL of solution at various concentrations

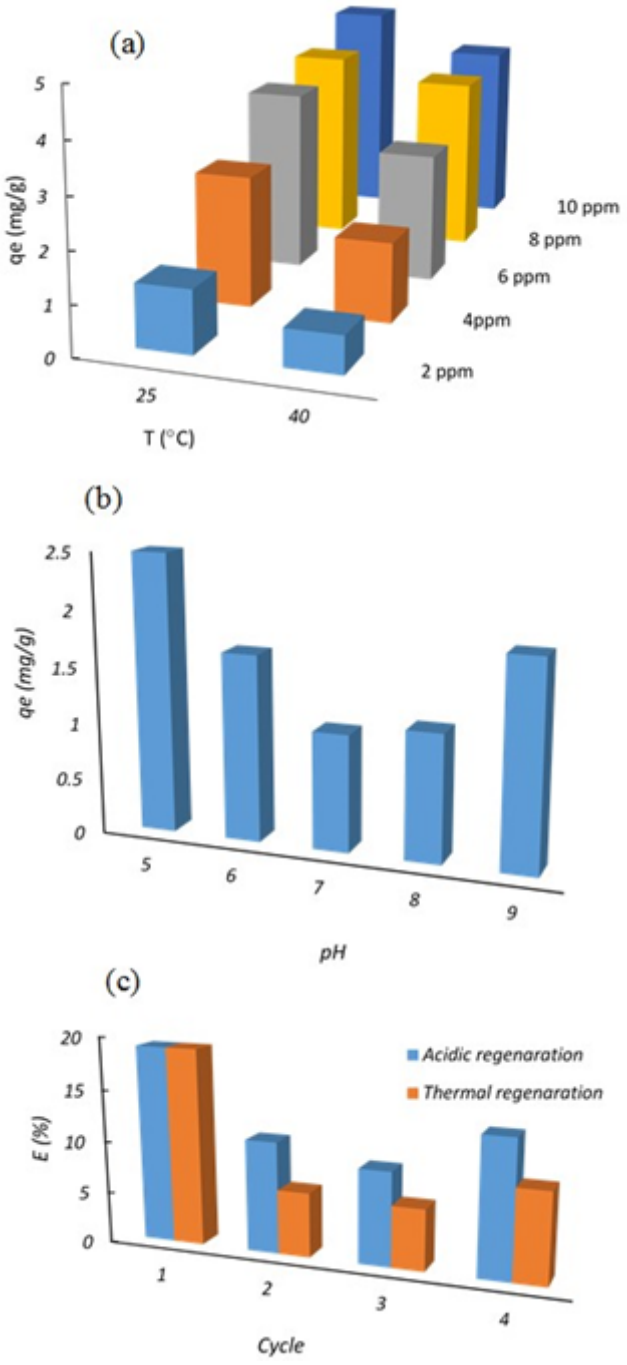

Figure 11

The effect of (a) the initial pH, (b) initial concentration of the solution on the adsorption capacity of methylene blue dye, and (c) regeneration and reuse experiment results for 0.02 g of adsorbent in 20 ml of solution